

SHOCKS AND SHELLS IN HOT STAR WINDS

A. FELDMEIER, J. PULS, C. REILE, A.W.A. PAULDRACH and
R.P. KUDRITZKI*

Universitäts-Sternwarte, Scheinerstr. 1, 81679 München, Germany

and

S.P. OWOCKI

Bartol Research Institute, Newark, Delaware 19716, USA

Abstract. Radiation-driven winds of hot, massive stars show *variability* in UV and optical line profiles on time scales of hours to days. *Shock heating* of wind material is indicated by the observed X-ray emission. We present time-dependent hydrodynamical models of these winds, where flow *structures* originate from a strong instability of the radiative driving. Recent calculations (Owocki 1992) of the unstable growth of perturbations were restricted by the assumptions of 1-D spherical symmetry and isothermality of the wind. We drop the latter assumption and include the energy transfer in the wind. This leads to a severe numerical shortcoming, whereby all radiative cooling zones collapse and the shocks become isothermal again. We propose a method to hinder this collapse. Calculations for dense supergiant winds then show: (1) The wind consists of a sequence of narrow and dense shells, which are enclosed by strong reverse shocks (with temperatures of 10^6 to 10^7 K) on their starward facing side. (2) Collisions of shells are frequent up to 6 to 7 stellar radii. (3) Radiative cooling is efficient only up to 4 to 6 R_* . Beyond these radii, cooling zones behind shocks become broad and alter the wind structure drastically: all reverse shocks disappear, leaving regions of *previously* heated gas.

Key words: Stars: early type – Stars: winds – Hydrodynamics – Instabilities

1. Introduction

The driving mechanism of OB star winds is the momentum transfer from the stellar radiation field to heavy metal ions, accomplished in numerous UV line transitions. Building upon the work by Lucy & Solomon (1970), Castor et al. (1975), and Abbott (1980, 1982), current wind models solve the stationary 1-D hydrodynamics (Pauldrach et al. 1986), including a full non-LTE treatment (Pauldrach 1987), the radiative transfer allowing for multiple scattering (Puls 1987), and an empirical shock emission in the EUV (Pauldrach et al. 1994). These models are able to predict the correct mass loss rates and terminal velocities, and to reproduce the complete UV line spectrum (Pauldrach et al. 1994).

A major restriction of these models is their assumption that the wind is *smooth and stationary*, whereas a wealth of observational evidence exists for wind structure and variability (the latter on time scales of hours to days). Among these are: “Discrete absorption components” (DACs) in unsaturated

* affiliated to Max-Planck-Institut für Astrophysik, 85740 Garching, Germany

P Cygni line profiles (Prinja & Howarth 1986; Henrichs 1988; Kaper 1993; Prinja & Fullerton 1994); broad and black absorption troughs (Lucy 1982; Puls et al. 1993; Prinja & Howarth 1986) and variability of the blue absorption edge (Henrichs 1991) in saturated UV P Cygni profiles. The X-ray emission from OB stars is discussed, e.g., by Hillier et al. (1993) and Cassinelli et al. (1994).

In the following we describe some recent efforts (Feldmeier 1993, 1995) in numerically modeling the non-linear evolution of initially small wind perturbations, which grow to mean flow scales due to the strong radiation-hydrodynamical instability of the wind (Lucy & Solomon 1970; Carlberg 1980; Abbott 1980; Lucy 1984; Owocki & Rybicki 1984, 1985). The correspondence of such wind structures to observed variability features is discussed in Puls et al. (1993, 1995). Our main interest here is the inclusion of the energy transfer in the wind, (1) to calculate the X-ray emission, and (2) to test the assumption of isothermality which underlies all supergiant wind models up to now (Owocki et al. 1988; Owocki 1991, 1995). Technical details of our approach are described in the latter papers and in Feldmeier (1993, 1995).

2. The wind model

Our present simulations are performed for a typical O supergiant with stellar parameters close to the ones of ζ Pup (O4If): $M = 42M_{\odot}$, $R_{*} = 19R_{\odot}$, $T_{\text{eff}} = 42,000$ K, $N_{\text{He}}/N_{\text{H}} = 0.16$ (Kudritzki et al. 1983). The wind parameters are $v_{\infty} = 2000$ km/s and $\dot{M} = 3 \cdot 10^{-6} M_{\odot}/\text{yr}$. The source function controlling the diffuse radiation force is assumed to be the one for purely geometric dilution of the photospheric radiation field, i.e., for an optically thin wind (Owocki 1991). For the radiative cooling function, we use the simple power law form $\Lambda = AN_{\text{e}}N_{\text{H}}T^{\alpha}$, with $\alpha = -1/2$ and $A = 1.64 \cdot 10^{-19}$ erg cm³ K^{1/2} s⁻¹. This is a reasonable approximation to the Raymond et al. (1976) cooling function from 10^5 to some 10^7 K. Finally, 3000 logarithmically spaced grid points from the photosphere up to $10R_{*}$ are used. The perturbation of the wind is due to a sound wave originating in the photosphere, with period 5000 s and amplitude 1%.

Wind model with collapsed cooling zones. Fig. 1 shows a snapshot of the wind structure 10 days after model start. The initially stationary wind (dashed line) is transformed into a sequence of very narrow and dense shells. The shells are enclosed by a strong reverse shock on their starward facing side, and by a compression wave or a forward shock on their outer side. (Which of both alternatives is actually realized cannot be decided conclusively from the still rather poor grid resolution). From about 4 to $5R_{*}$ on, the reverse shocks become weaker with growing distance. The (main) reason is that the instability vanishes with vanishing velocity gradient. Beyond about $5R_{*}$ the

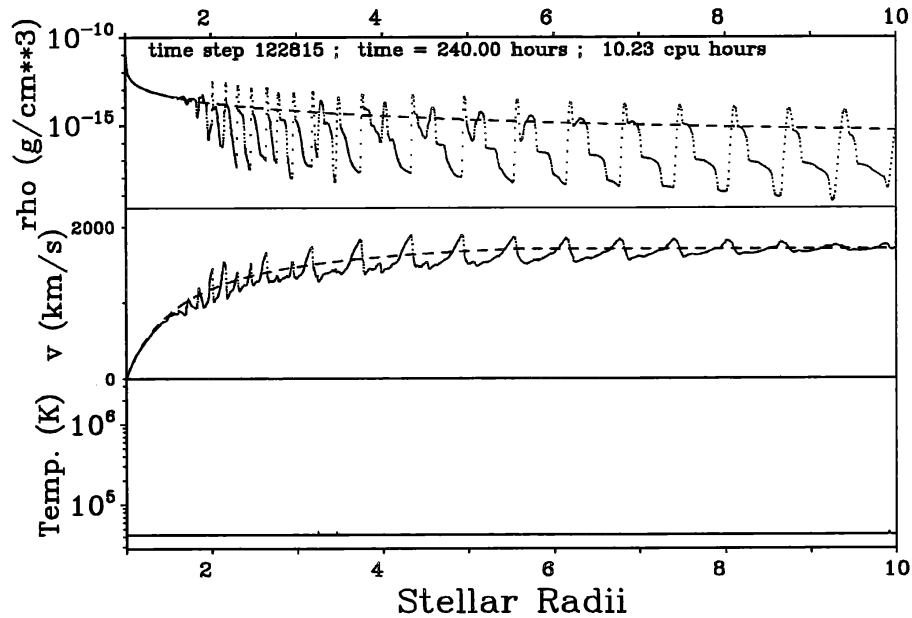


Fig. 1. Snapshot of the wind 10 days after model start. The values of ρ , v , and T at each grid point are plotted. Dashed line: stationary start model.

wind structure is periodic, whereas at lower radii it appears to be chaotic. However, the latter behavior results only from the creation of 3 or 4 shells per cycle of the sound wave, where these shells collide and merge with each other. To demonstrate the periodicity of the wind at all radii, Fig. 2 shows a grey-scale rendition of the temporal power spectrum of the velocity, plotted vs. frequency for the fixed locations $r = n R_*$, $n = 1, \dots, 10$. In addition to the frequency f of the sound wave, the first 40 to 50 harmonic overtones of f appear at $3 R_*$. They are excited by the nonlinear steepening of the sound wave due to the wind instability. The overtones die out with growing distance from the star. Besides these overtones, no other signal is evident in Fig. 2.

This behaviour is different in models with a large amplitude of the sound wave, and also in models without any explicit perturbation of the wind, i.e., with self-excited structure. In both of these cases, continuous intervals of frequencies are excited (the reasons for this differing behaviour are still under debate, cf. Feldmeier 1995; Owocki & Feldmeier, in preparation), which *may* indicate *turbulent* behaviour of the wind (Burgers 1950; Tatsumi & Tokunaga 1974). Observational evidence for compressible turbulence in Wolf-Rayet star winds is found from the spectral size distribution of wind blobs (Moffat 1994).

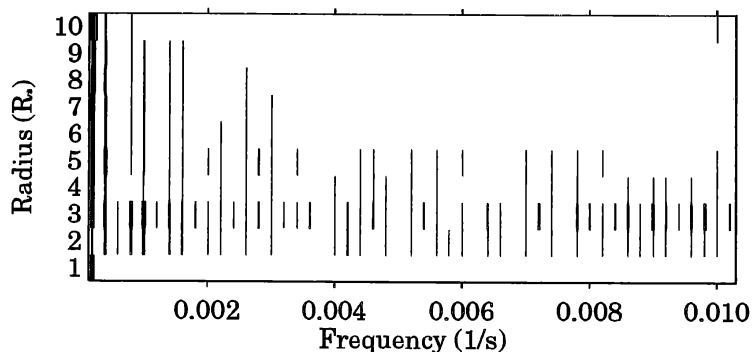


Fig. 2. Grey scale rendition of the temporal power spectrum of the velocity $v(t)$, sampled over 48 cycles of the sound wave, at several fixed locations in the wind. In addition to the frequency of the sound wave (broad line at the left edge of the figure), its first ≈ 40 to 50 harmonic overtones are excited.

Finally, from the velocity jumps in Fig. 1 one expects post-shock temperatures of order 10^6 K. *Contrary to this, no hot material is seen in Fig. 1.* Let us now consider the reason for this discrepancy.

The collapse of radiative cooling zones. Due to the global thermal instability (Langer et al. 1981; Chevalier & Imamura 1982; Falle, this proceedings), the radiative cooling zones behind strong shocks contract and expand periodically. We claim, that *during the contractional phase the cooling zone may fall below the grid resolution*, whereby the numerical scheme “forgets” about the existence of the cooling zone, and an *isothermal shock* is left. The reversible oscillation of the cooling zone has turned into an irreversible collapse. This is demonstrated in Fig. 3 for a test calculation with gas streaming supersonically against a wall (located at $x = 0$). The left panel shows a calculation on a grid fine enough to resolve the thermal oscillation, and the middle panel the same calculation on a coarse grid, where the cooling zone collapses at the wall.

To hinder this collapse, we propose to modify the cooling function at low temperatures. More specifically, we chose a stable cooling exponent $\alpha = +2$ below a temperature T_{swi} . The stabilizing influence of the low temperature regime can then hinder the collapse altogether. This is seen in the right panel of Fig. 3 for a calculation on the same coarse grid as in the mid panel. Since (1) only the *hot* gas emits X-rays, and (2) again the *hot* gas, by its very inefficient radiative cooling, fixes almost alone the total extent of the cooling layer, this modification of Λ at *low* temperatures should have an only minor influence on the interesting wind physics.

There is a second, purely numerical cause for the collapse of cooling zones, termed “advective diffusion”. For a discussion of this defect (which is also hin-

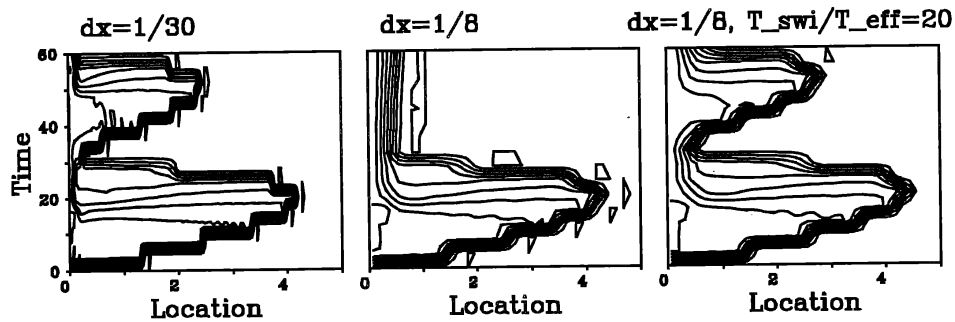


Fig. 3. Global thermal instability oscillation (in terms of iso-velocity contours) on a fine grid (resolved; left panel), a coarse grid (collapsed; mid panel), and on the coarse grid using our modified cooling function (right panel, see text).

dered by the above modification of the cooling function), we refer to Cooper (1994) and Feldmeier (1995).

Wind model with resolved cooling zones. Fig. 4 shows a wind snapshot, where now the cooling function is modified in the described manner below $T_{\text{swi}} = 10 T_{\text{eff}}$. Hot gas of order 10^6 K is present, and cooling zones behind strong shocks are resolved. Up to about $4 R_*$, the structure is very similar to the one displayed in Fig. 1: the cooling zones are short compared to shell-shell distances, *confirming the assumption of dynamical isothermality in this region.*

However, beyond $4 R_*$ this model shows striking differences to Fig. 1. Within the sequence marked with (a) to (d) in Fig. 4, *all reverse shocks are destroyed*: The intershell material (being fed into the shells) is depleted, which leads to a broadening of the cooling layers. Since the material at the cold edge of the cooling zone is very dense and therefore very inert, this broadening occurs by driving the reverse shock into the preshock gas (i.e. to the left). Hereby, the shock encounters material of always lower velocity, and the shock jump becomes smaller until it finally vanishes. Thus, the hot material at large radii ($> 5 R_*$) is the left-over from *previous* shock heating at smaller radii. This gas cools away steadily due to radiative energy losses and spherical expansion on its further advection through the wind.

3. Conclusions

The observational consequences of these results for the X-ray emission from hot stars have now to be analyzed. This work is presently under way in our group. Since only the hard X-ray component ($E \gtrsim 1$ keV) of ζ Pup stems from radii smaller than $10 R_*$ (Hillier et al. 1993), we can conclude tentatively

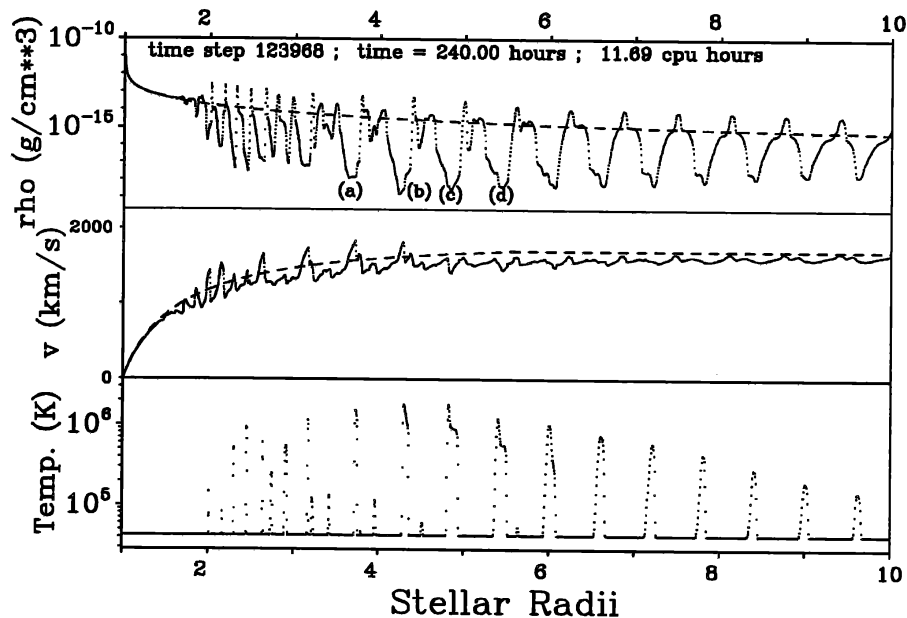


Fig. 4. Snapshot of the wind using a modified radiative cooling function below $T_{\text{swi}}/T_{\text{eff}} = 10$.

that only this component should (partially) originate from radiative shocks, whereas the soft X-rays far out in the wind should originate from “old” hot gas. However, it is not clear at present if the latter material is not too rarefied in our models to produce an observable X-ray flux. Finally, the maximum temperatures of order 10^6 K in Fig. 4 are too small to account for the ROSAT observations of ζ Pup, which instead indicate temperatures ranging up to 3 to $4 \cdot 10^6$ K. However, hotter material is more readily produced in models with larger photospheric wind perturbations. The principal shock destruction occurs in the same way as described above, but is shifted now to somewhat larger radii ($\approx 6 R_*$). Interestingly, the volume filling factor of hot material at large radii can reach $\approx 60\%$ then (Feldmeier 1995). Assuming a density depletion factor of 100 of this hot material compared with stationary wind densities, this results in a filling factor (relative to the stationary wind) of $\approx 0.6\%$, not too different from the few % derived by Hillier et al. (1993).

Acknowledgements

We thank A. Fullerton and S. Haser for interesting discussions. A.F. and A.P. were supported by the DFG in the “Gerhard-Hess-Programm” under contracts Pa 477/1-1 and 1-2. C.R. was supported by the BMFT under con-

tract 05-2MU114(7). S.P.O. acknowledges partial support from NSF grant AST 91-15136 and from NASA grant NAGW-2624. The calculations were performed on a Cray Y-MP at the Leibniz-Rechenzentrum in München.

References

- Abbott, D.C.: 1980, *Astrophys. J.*, **242**, 1183.
 Abbott, D.C.: 1982, *Astrophys. J.*, **259**, 282.
 Burgers, J.M.: 1950, *Proc. Acad. Sci. Amst.*, **53**, 247, 393, 718, 732.
 Carlberg, R.G.: 1980, *Astrophys. J.*, **241**, 1131.
 Cassinelli, J.P., Cohen, D.H., MacFarlane, J.J., Sanders, W.T., Welsh, B.Y.: 1994, *Astrophys. J.*, **421**, 705.
 Castor, J.I., Abbott, D.C., Klein, R.I.: 1975, *Astrophys. J.*, **195**, 157.
 Chevalier, R.A., Imamura, J.N.: 1982, *Astrophys. J.*, **261**, 543.
 Cooper, R. G. 1994, PhD thesis, University of Delaware.
 Feldmeier, A.: 1993, PhD thesis, Universität München.
 Feldmeier, A.: 1995, *Astron. Astrophys.*, in press.
 Henrichs, H.F.: 1988, in Conti, P.S., Underhill A.B., ed(s)., *O Stars and Wolf-Rayet Stars*, NASA SP-497: Washington, D.C., 199.
 Henrichs, H.F.: 1991, in Baade, D., ed., *Rapid Variability of OB-Stars: Nature and Diagnostic Value*, ESO Conf. Proc. No. 36: Garching, 199.
 Hillier, D.J., et al.: 1993, *Astron. Astrophys.*, **276**, 117.
 Kaper, L.: 1993, PhD thesis, Amsterdam.
 Kudritzki, R.P., Simon, K.P., Hamann, W.R.: 1983, *Astron. Astrophys.*, **118**, 245.
 Langer, S.H., Chanmugam, G., Shaviv, G.: 1981, *Astrophys. J.*, **245**, L23.
 Lucy, L.B., 1982: *Astrophys. J.*, **255**, 278.
 Lucy, L.B., 1984: *Astrophys. J.*, **284**, 351.
 Lucy, L.B., Solomon, P.M.: 1970, *Astrophys. J.*, **159**, 879.
 Moffat, A.F.J.: 1994, in Klare, G., ed., *Reviews in Modern Astronomy 7*, Astronomische Gesellschaft: Hamburg, 51.
 Owocki, S.P.: 1991, in Crivellari, L., Hubeny, I., Hummer, D.G., ed(s)., *Stellar Atmospheres: Beyond Classical Models*, Kluwer: Dordrecht, 235.
 Owocki, S.P.: 1992, in Heber, U., Jeffery, S., ed(s)., *Atmospheres of Early-Type Stars*, Springer: Heidelberg, 393.
 Owocki, S.P.: 1995, in Moffat, A.F.J., et al., ed(s)., *Instability and Variability of Hot Star Winds*, Kluwer: Dordrecht, in press.
 Owocki, S.P., Rybicki, G.B.: 1984, *Astrophys. J.*, **284**, 337.
 Owocki, S.P., Rybicki, G.B.: 1985, *Astrophys. J.*, **299**, 265.
 Owocki, S.P., Castor, J.I., Rybicki, G.B.: 1988, *Astrophys. J.*, **335**, 914.
 Pauldrach, A.: 1987, *Astron. Astrophys.*, **183**, 295.
 Pauldrach, A., Puls, J., Kudritzki, R.P.: 1986, *Astron. Astrophys.*, **164**, 86.
 Pauldrach, A.W.A., Kudritzki, R.P., Puls, J., Butler, K., Hunsinger, J.: 1994, *Astron. Astrophys.*, **283**, 525.
 Prinja, R.K., Fullerton, A.W.: 1994, *Astrophys. J.*, **426**, 345.
 Prinja, R.K., Howarth, I.D.: 1986, *Astrophys. J. Suppl.*, **61**, 357.
 Puls, J.: 1987, *Astron. Astrophys.*, **184**, 227.
 Puls, J., Owocki, S.P., Fullerton, A.W.: 1993, *Astron. Astrophys.*, **279**, 457.
 Puls, J., Feldmeier, A., Springmann, U., Owocki, S.P., Fullerton, A.W.: 1995, in Moffat, A.F.J., et al., ed(s)., *Instability and Variability of Hot Star Winds*, Kluwer: Dordrecht, in press.
 Raymond, J.C., Cox, D.P., Smith, B.W.: 1976, *Astrophys. J.*, **204**, 290.
 Tatsumi, T., Tokunaga, H.: 1974, *J. Fluid Mech.*, **65**, 581.